

# Photoinduced Charge Separation and Recombination Processes in CdSe Quantum Dot and Graphene Oxide Composites with Methylene Blue as Linker

Pengtao Jing,<sup>†,§</sup> Wenyu Ji,<sup>†</sup> Xi Yuan,<sup>†,‡</sup> Michio Ikezawa,<sup>§</sup> Ligong Zhang,<sup>†</sup> Haibo Li,<sup>||</sup> Jialong Zhao,<sup>\*,†,||</sup> and Yasuaki Masumoto<sup>\*,§</sup>

<sup>†</sup>State Key Laboratory of Luminescence and Applications, Changchun Institute of Optics, Fine Mechanics and Physics, Chinese Academy of Sciences, 3888 Eastern South Lake Road, Changchun 130033, China

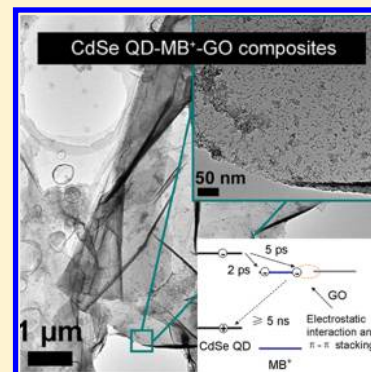
<sup>‡</sup>University of Chinese Academy of Sciences, Beijing 100039, China

<sup>§</sup>Institute of Physics, University of Tsukuba, Tsukuba, Ibaraki 305-8571, Japan

<sup>||</sup>Key Laboratory of Functional Materials Physics and Chemistry of the Ministry of Education, Jilin Normal University, Siping 136000, China

## Supporting Information

**ABSTRACT:** The charge separation and recombination processes between CdSe quantum dot (QD) and graphene oxide (GO) composites with linking molecule methylene blue (MB<sup>+</sup>) were studied by femtosecond transient absorption spectroscopy. Anchoring MB<sup>+</sup> molecules on GO results in significant changes in steady-state and transient absorption spectra, where the exciton dissociation time in the CdSe QD-MB<sup>+</sup>-GO composite was determined to be 1.8 ps. Surprisingly, the ground state bleaching signal increased for MB<sup>+</sup>-GO complex was found to be 5.2 ps, in relation with electron transfer from QD to GO. On the other hand, the strong electronic coupling between MB<sup>•</sup>-GO radical and GO prolonged charge recombination process ( $\geq 5$  ns) in QD-MB<sup>+</sup>-GO composites. Charge separation and recombination processes at the interface between semiconductor QDs and graphene can thus be modulated by the functionalized dye molecules.



**SECTION:** Physical Processes in Nanomaterials and Nanostructures

Inorganic–organic hybrid materials, especially semiconductor quantum dots (QDs) and organic conjugated molecules, demonstrate potential applications in solar cells<sup>1–3</sup> and light emitting diodes<sup>4,5</sup> due to the size-tunable optoelectronic properties of QDs and the flexible solution fabrication of the composite. The multiexciton generation (MEG) has been observed in PbS, PbSe, CdSe, and Si QDs,<sup>6–10</sup> and the effects of MEG have been demonstrated in QD based photovoltaic devices,<sup>11,12</sup> despite the casted doubts, e.g., in the reports of Nair et al.<sup>13</sup> and Ben-Lulu et al.<sup>14</sup> In this aspect, ultrafast study indicated that the charge separation from the QDs to organic electron acceptor molecules or inorganic metal oxide (methylviologen, methylene blue, ZnO, or TiO<sub>2</sub>, etc.) is fast enough to ensure the extraction of multiple excitons before their Auger recombination.<sup>15–24</sup> For example, in type I CdSe/ZnS core/shell QDs absorbed with anthraquinone (AQ) molecules, the charge separation and recombination rates decrease exponentially with the increase of the shell thickness.<sup>21</sup> Zhu et al. found that in quasi-type II CdSe/CdS core–shell QDs, ultrafast charge separation, ultraslow charge recombination and slow exciton Auger annihilation could be realized.<sup>19</sup> Ultrafast dynamics of multiple electron transfer from CdSe QDs to a ZnO film was found to be significantly sensitive to the

QD size ascribed to the competition between electron injection and Auger recombination.<sup>21</sup> In a word, the charge separation and recombination can be tailored by core/shell structures, shapes, and sizes of QDs and their surface ligands. To improve the performance of QD based solar cells, a fast transportation and efficient charge collection are essential to avoid electron and hole recombination in QDs. However, employing multi-excitions mechanism to improve the performance of QD based photovoltaic devices remains a challenge.

On the other hand, the unique electronic properties of graphene ensure the ability of transporting electrons along its two-dimensional (2D) network, showing an attractive perspective of applications in QD-based photovoltaic devices.<sup>24–31</sup> Chemically derived graphene oxide (GO) with functional groups such as –OH, –COOH, and epoxide as anchoring points can be further modified with organic molecules, semiconductor QDs, and metal nanoparticles.<sup>32–42</sup> Recently, Lightcap et al. investigated electron and energy transfer processes from CdSe QDs to GO or reduced graphene

**Received:** July 13, 2013

**Accepted:** August 13, 2013

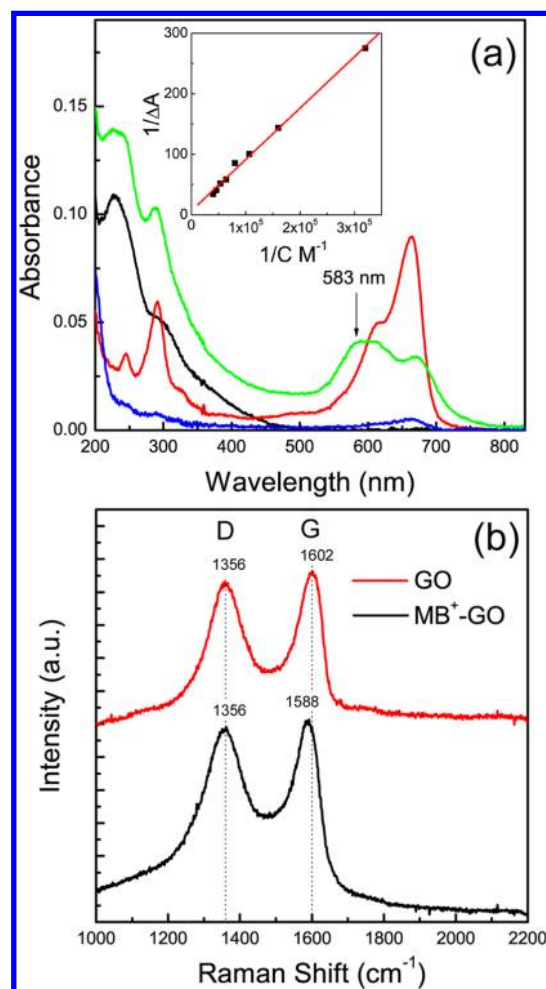
**Published:** August 13, 2013

oxide (RGO).<sup>29</sup> However, the charge separation rates ( $\sim 1$  ns<sup>-1</sup>) from QDs to GO and to RGO were slower than Auger recombination rate ( $\sim 10$ – $100$  ns<sup>-1</sup>) of multiexcitons.<sup>29,44</sup> The positively charged aromatic dyes could be noncovalently functionalized on graphene or GO via  $\pi$ - $\pi$  stacking, van der Waals, and electrostatic interaction.<sup>33</sup> It was confirmed from ultrafast transient absorption (TA) spectroscopy that the charge transfer interaction occurred in the complex of 5,10,15,20-tetrakis(1-methyl-4-pyridinio) porphyrin-tetra-(p-toluenesulfonate) (TMPyP) and RGO.<sup>37</sup> The interfacial electron transfer rate from 9-phenyl-2,3,7-trihydroxy-6-fluorone (PF) to nanometer-sized GO was determined to be  $10^{11}$  s<sup>-1</sup> by the direct monitoring of the PF radical cation.<sup>38</sup> So far, fundamental photophysical processes in hybrid nanomaterials of semiconductor QDs and dye modified graphene have not been completely revealed.

In this work, we studied the charge separation and recombination processes in CdSe QD-MB<sup>+</sup>-GO composites from femtosecond transient absorption (TA) spectroscopy. Methylene blue (MB<sup>+</sup>) molecules were attached on GO via electrostatic interaction and  $\pi$ - $\pi$  stacking to realize the functionalization of graphene. Ultrafast electron separation from CdSe QDs to MB<sup>+</sup>-GO complex and slow back electron-hole recombination between the radical and the QD have been demonstrated.

Figure 1a shows the absorption spectra of MB<sup>+</sup> molecules and MB<sup>+</sup>-GO complex in water. Methylene green (MG<sup>+</sup>) was reported to be noncovalently functionalized on chemically reduced graphene oxide.<sup>39</sup> Molecular structure of MB<sup>+</sup> is similar to that of MG<sup>+</sup>. The absorption peaks of MB<sup>+</sup> attached on GO are weak and broad - a feature of  $\pi$ - $\pi$  stacking and electrostatic interaction between MB<sup>+</sup> and GO, similar to those observed in MB<sup>+</sup>-carbon nanotube (CNT) nanocomposite.<sup>39,46,47</sup> The Benesi-Hildebrand method was adopted to study the interaction of MB<sup>+</sup> and GO in water.<sup>37</sup> The apparent association constant was obtained to be  $7.7 \times 10^3$  M<sup>-1</sup>, as seen in the inset of Figure 1a. After filtration, the absorption peak of the MB<sup>+</sup>-GO complex almost disappeared, indicating that a large proportion of MB<sup>+</sup> molecules were attached on GO sheets. The detail method is described in Supporting Information. Moreover, MB<sup>+</sup>-GO complex shows a new absorption peak around 583 nm. Under 620 nm excitation, the photoluminescence (PL) of the MB<sup>+</sup>-GO complex was quenched by 93% compared to that of MB<sup>+</sup> molecules (Figure S3a). The PL quenching was attributed to electron transfer or energy transfer from MB<sup>+</sup> to GO.<sup>37-42</sup> On the other hand, the G band of GO in the Raman spectrum shifts to 1588 cm<sup>-1</sup> from 1602 cm<sup>-1</sup> after adsorption of MB<sup>+</sup> molecules (Figure 1b). This demonstrates that cationic dye molecule influences the in-phase of bond-stretching vibration of pairs of C sp<sup>2</sup> atoms.<sup>48,49</sup> Meanwhile, the frequency shift of the stretching mode  $\nu$ (C=C) of double bonds was also observed in Fourier transform infrared (FTIR) spectra in Figure S3b.<sup>46</sup> However, the D band and  $I_D/I_G$  ratio of GO and MB<sup>+</sup>-GO complex are still around 1356 cm<sup>-1</sup> and 0.93–0.94, respectively, indicating that MB<sup>+</sup> dye molecules do not change the degree of disorder of GO sheets.<sup>48,49</sup>

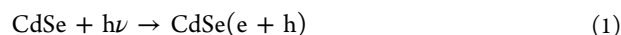
CdSe-MB<sup>+</sup>-GO composite was prepared by the bottom-up method as described in the experimental section. Figure 2a shows the transmission electron microscope (TEM) images of CdSe QD-MB<sup>+</sup>-GO composites. GO is micrometer-sized 2D network. Due to  $\pi$ - $\pi$  stacking and electrostatic interaction between MB<sup>+</sup> and GO, CdSe QDs were successfully anchored



**Figure 1.** (a) Absorption spectra of MB<sup>+</sup> molecules (black solid line), MB<sup>+</sup>-GO complex (red solid line), GO (green solid line), and MB<sup>+</sup>-GO complex after filtration (blue solid line) in water. Inset: The inverse of  $\Delta A$  at 470 nm as a function of the inverse of MB<sup>+</sup> concentration. The red line represents the fitted line via Benesi-Hildebrand method. (b) Raman spectra of GO and the MB<sup>+</sup>-GO complex.

on the GO surface via positively charged aromatic dye molecules (MB<sup>+</sup>) as linkers.<sup>40</sup> TEM images of QDs, QD-MB<sup>+</sup> and QD-GO complex (Figure S4). It is noticed that some QDs can not be anchored on GO sheet in QD-GO complex without MB<sup>+</sup> molecules, as seen in Figure S4 (e-h). Figure 2b shows the absorption spectra of CdSe QDs, QD-MB<sup>+</sup>, and QD-MB<sup>+</sup>-GO composites. It is known that absorption peaks at 573, 542, and 480 nm of CdSe QDs correspond to the optical transitions of  $1S(e)-1S_{3/2}(h)$ ,  $1S(e)-1S_{1/2}(h)$ , and  $1P(e)-1S_{3/2}(h)$ , respectively.<sup>43</sup> The two additional peaks at 670 and 620 nm in Figure 2b are due to the absorption of MB<sup>+</sup> molecules on the QD.<sup>17</sup> In QD-MB<sup>+</sup>-GO composites, the red-shift of the first exciton absorption peak for CdSe QDs was observed, which is attributed to the slight aggregation of the QDs on the GO surface, as seen in Figure 2.

Femtosecond TA spectroscopy has been used to study charge separation and recombination processes between CdSe QD and MB<sup>+</sup> molecule or MB<sup>+</sup>-GO complex. The expected processes in these systems are summarized as follows:<sup>15,17,29</sup>



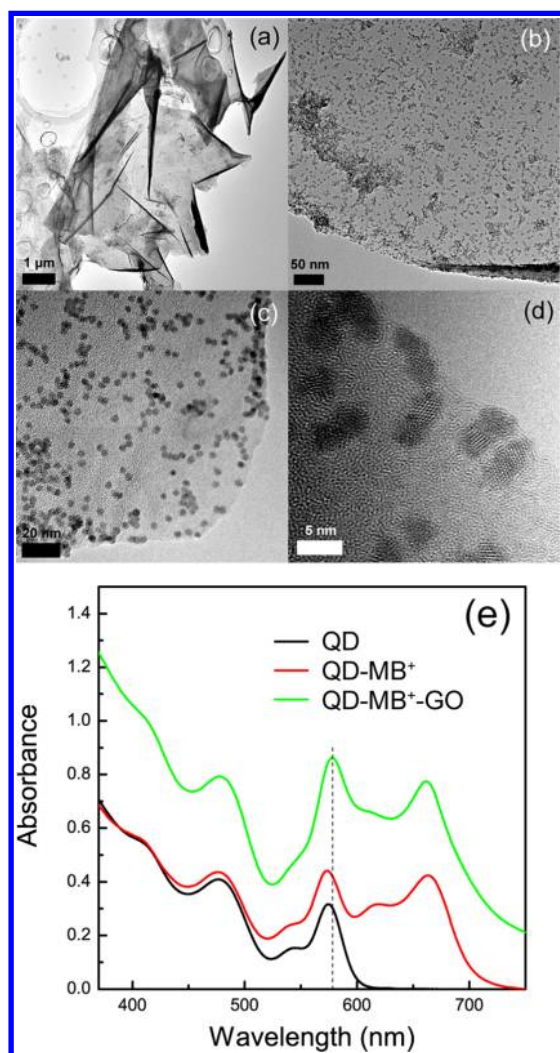
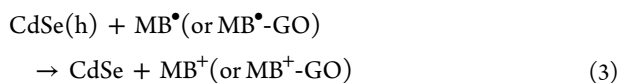
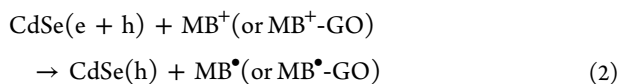


**Figure 2.** TEM images of CdSe QD-MB<sup>+</sup>-GO composite with different enlargement. The scale bars are (a) 1 μm, (b) 50 nm, (c) 20 nm, (d) 5 nm, respectively. (e) Absorption spectra of CdSe QDs (black solid line), CdSe QDs with MB<sup>+</sup> (red solid line), and MB<sup>+</sup>-GO (green solid line) in toluene.



Process (1) reflects that CdSe QD absorbs a photon to generate an electron–hole pair (exciton) in the QD.<sup>43,44</sup> An electron and a hole are separated from each other at the QD-MB<sup>+</sup> (or QD-MB<sup>+</sup>-GO) interface.<sup>15–21</sup> At the same time, the MB<sup>+</sup> (or MB<sup>+</sup>-GO) captures an additional electron, inducing ground state bleaching (GSB) signal.<sup>17,20</sup> Finally, the captured electron on MB<sup>•</sup> (or MB<sup>•</sup>-GO) radical recombines with the remained hole in the QD.<sup>17,20</sup>

The TA spectra of CdSe QDs, QD-MB<sup>+</sup>, and QD-MB<sup>+</sup>-GO composites taken at different delay times after 400 nm excitation are shown in Figure 3. Three TA bleaching peaks at 573, 542, and 480 nm are observed in CdSe QDs, corresponding to the optical transition of 1S(e)–1S<sub>3/2</sub>(h), 1S(e)–1S<sub>1/2</sub>(h), and 1P(e)–1S<sub>3/2</sub>(h), respectively.<sup>43</sup> The TA

bleaching signal can be attributed to the state filling of 1S and 1P electron levels in CdSe QDs.<sup>43,44</sup> The photoinduced absorption (PA) features at 600 and 510 nm show a red-shift compared with 1S and 1P transitions because of existence of the biexciton and a trapped-carrier-induced dc Stark effect.<sup>43</sup> As reported in Lian's previous work, MB<sup>+</sup> molecules act as electron acceptor for CdSe QDs, which induces ultrafast charge separation at the interface of QDs and MB<sup>+</sup> molecules.<sup>17</sup> As seen in Figure 3b, the TA bleaching signals of 1S and 1P exciton states decay very fast, indicating fast electron transfer from these states to MB<sup>+</sup> molecules. Further, two additional bleaching peaks at 620 and 675 nm are observed in TA spectra of QD-MB<sup>+</sup> composite, due to the ground state filling of MB<sup>+</sup> molecules after electron injection.<sup>17</sup> As seen in Figure 3c, the TA bleaching signals of 1S and 1P exciton states of CdSe QDs also decay very fast, indicating fast exciton dissociation in CdSe QDs. Additionally, the disappearance of the bleaching peaks at 620 and 675 nm demonstrates the effect of GO on MB<sup>+</sup> molecules.

The amplitude of the bleaching signal at 573 nm reflects the population of 1S exciton state in CdSe QDs. The normalized TA bleaching signals at 573 nm for CdSe QD, CdSe QD-MB<sup>+</sup>, and CdSe QD-MB<sup>+</sup>-GO composites as a function of time are shown in Figure 3d. The amplitudes in QD-MB<sup>+</sup> and QD-MB<sup>+</sup>-GO composites decay very fast, indicating electron transfer is an additional de-excitation pathway for 1S exciton in QDs. The fitted decay lifetimes of CdSe QDs with MB<sup>+</sup> and MB<sup>+</sup>-GO are determined to be 1.6 and 1.8 ps, which are faster than that of the QDs alone. The fitted results are summarized in Table S1. The electron separation time is faster than the multiexciton annihilation lifetime of about 10–100 ps, indicating that the MB<sup>+</sup> molecule and MB<sup>+</sup>-GO complex can dissociate excitons from QDs.<sup>17,44</sup> However, the electron transfer or energy transfer rate from QDs to GO sheet without MB<sup>+</sup> linker is slower than that in QD-MB<sup>+</sup> or QD-MB<sup>+</sup>-GO complex, as shown in Figure S5, Tables S1 and S2. Additionally, it is noted that the decay profile of QD-MB<sup>+</sup>-GO composite shows a slow component, which may be attributed to GSB signal of MB<sup>+</sup>-GO complex, as discussed in the following section.

Electron from exciton dissociation should be injected into MB<sup>+</sup> molecule or MB<sup>+</sup>-GO complex to form the radical, inducing the ground-state bleaching of electron acceptor. Figure 4a shows TA spectral difference of CdSe QDs connected with MB<sup>+</sup> molecules and MB<sup>+</sup>-GO complex. The photoinduced electron transfer results in the MB<sup>+</sup> ground-state bleaching observed at 620 and 675 nm, as seen in Figure 4a. However, these bleaching peaks disappear in TA spectra of QD-MB<sup>+</sup>-GO composite while a broad bleaching signal peaked at 583 nm appears around 520–640 nm, as seen in Figure 4a. The signal is attributed to MB<sup>+</sup>-GO complex, corresponding to the new peak in the steady-state absorption spectrum when GO is mixed into QD-MB<sup>+</sup> complex solution. The steady-state (Figure 2e) and TA peaks (Figure 4a) of CdSe QDs show a red-shift compared to that of QD-MB<sup>+</sup> composite, caused by aggregation of the QDs on GO sheet, as seen in TEM images in Figure 2.

In order to quantitatively investigate charge separation and recombination processes in QD-MB<sup>+</sup> and QD-MB<sup>+</sup>-GO composites, we need to analyze time dependent GSB signals of MB<sup>+</sup> molecules and MB<sup>+</sup>-GO complex. As seen in Figure 4b, the generation and decay of the GSB signal in the QD-MB<sup>+</sup> complex probed at 675 nm (as seen by arrow in Figure 4a) are attributed to the electron transfer from QD to MB<sup>+</sup> and charge recombination of electron on MB<sup>•</sup> radical with a hole in the

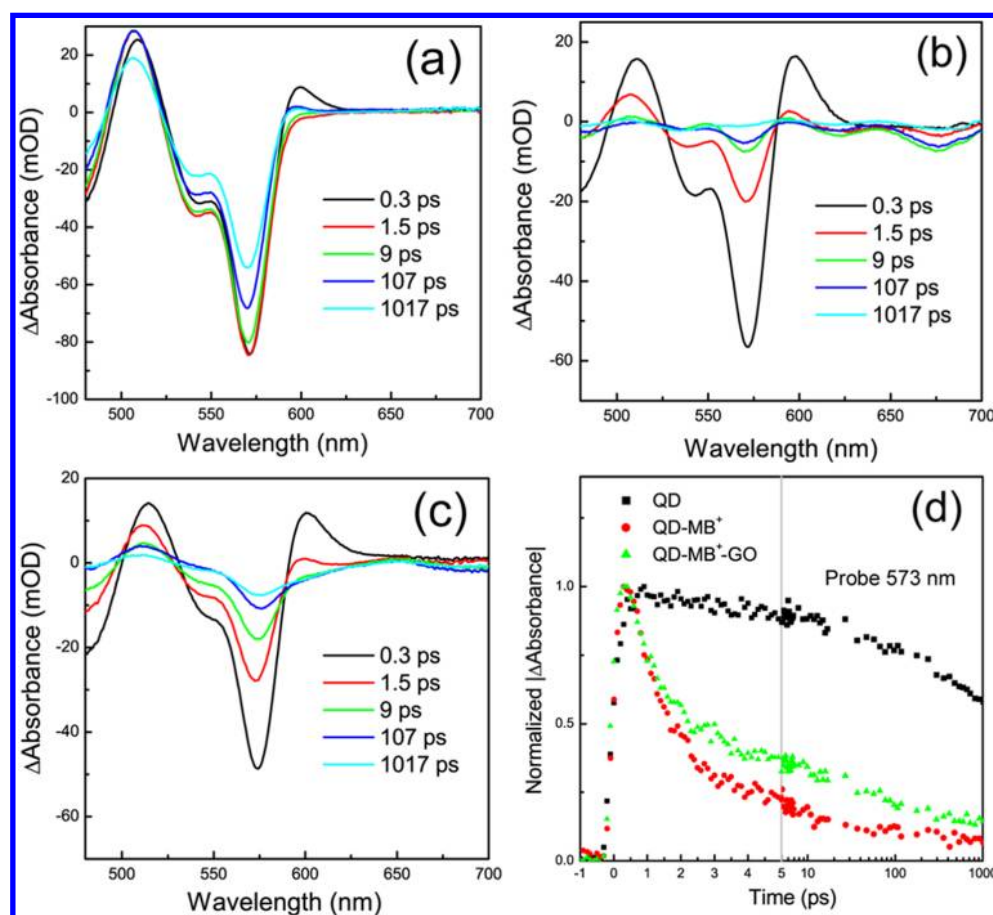


**Figure 3.** TA spectra of CdSe QDs (a), CdSe QDs with MB<sup>+</sup> molecules (b), and with MB<sup>+</sup>-GO complex (c) at different delay times after excitation. (d) TA kinetic traces in CdSe QDs (black squares), CdSe QDs with MB<sup>+</sup> molecules (red cycles) and MB<sup>+</sup>-GO complex (green triangles). The probe wavelength is 573 nm. Left is linear scale and right is logarithmic scale in (d).

QD, as described in processes 2 and 3. The time behavior of the bleaching monitored at 675 nm follows biexponential function with a rise and a decay component. The rise and decay times are determined to be 1.8 and 647 ps, respectively. The recombination lifetime is faster than that in the previous report,<sup>17</sup> which is related to the different surface passivation of core QDs.

Some unknown photophysical processes in QD-MB<sup>+</sup>-GO composite may contain in the time evolution of new bleaching feature. TA kinetic trace in QD-MB<sup>+</sup>-GO probed at 583 nm shows an inflection point around 5 ps, as seen in Figure S6. This inflection is related to the GSB signal formation of MB<sup>+</sup>-GO complex. However, this TA kinetic trace contains the bleaching signal of the 1S exciton state for CdSe QDs. To avoid the influence of the bleaching signal of CdSe QDs, the time-dependent GSB signal of QD-MB<sup>+</sup>-GO was probed at 610 nm (Figure 4c). The PA signal decays very fast with a lifetime of 0.5 ps, as determined from the fitting (Figure 4c). The GSB rise time is about 5.2 ps, which is longer than the charge separation lifetime detected from the CdSe 1S exciton state bleaching signal, as seen in Figure S7. This result implies that an additional electron transfer process happens after exciton dissociation. Although the reduction potentials of MB<sup>+</sup> (+0.038 V vs NHE) and GO (+0.04 V vs NHE) are close to each other, the PL of MB<sup>+</sup> is significantly quenched by attaching MB<sup>+</sup> on GO, suggesting electron and/or energy transfer from MB<sup>+</sup> to GO.<sup>17,45</sup> Consequently, the captured electron on MB<sup>+</sup> radical can move from the QD to GO via MB<sup>+</sup>

molecule as a bridge, inducing the enhanced formation time of MB<sup>+</sup>-GO radical. In the previous report, the interaction energies ( $\Delta E$ ) of the complex of MB<sup>+</sup> cation with a graphene sheet were estimated to be  $-45.0$  and  $-43.1$  kcal/mol for "armchair" and "zigzag" types, respectively. These values are obviously larger than that of MB<sup>+</sup>-CNT complex.<sup>47</sup> The lowest unoccupied molecular orbital (LUMO) of MB<sup>+</sup>-CNT complex is delocalized over both the MB<sup>+</sup> cation and the nanotube in the complex with metallic type "armchair" CNT and localized on the cation in its complex with semiconducting "zigzag" CNT.<sup>47</sup> Furthermore, if the captured electron is far away from the QD surface, the charge recombination lifetime in QD-MB<sup>+</sup>-GO composite will become longer than that in QD-MB<sup>+</sup> composite. The electron-hole recombination lifetime in the QD-MB<sup>+</sup>-GO composite is determined to be larger than 5 ns, in good agreement with the above prediction. Generally, the long charge recombination lifetime can be reached by reducing the electronic coupling strength, which is dependent on the overlap of the LUMO of MB<sup>+</sup>-GO radicals with the hole wave function in the valence band of QDs, for example coating a ZnS or CdS shell on the CdSe core.<sup>19,21</sup> In our experiment, the captured electron on MB<sup>+</sup> radical is strongly influenced by GO sheets via  $\pi$ - $\pi$  stacking and electrostatic interaction. Therefore, the electron on MB<sup>+</sup> radical is prone to transfer from the QD to the GO, resulting in the weakened electronic coupling strength between the radical and the QD. For this reason, the long charge recombination lifetime ( $\geq 5$  ns) is reasonable, which is consistent with the enhanced radical formation time (5.2 ps).

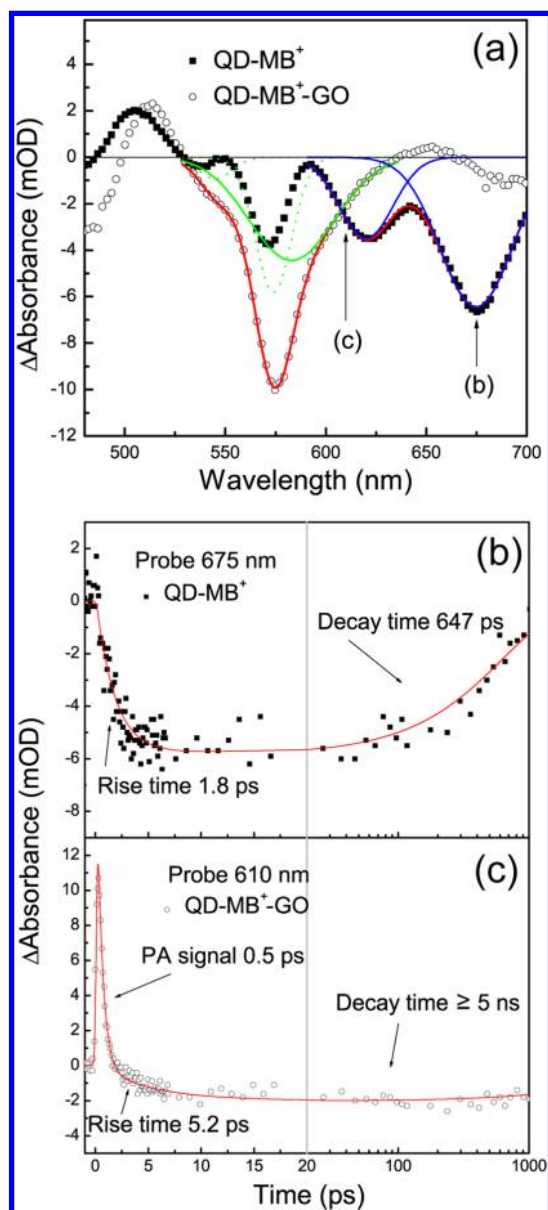


**Figure 4.** (a) TA spectra of CdSe QDs with MB<sup>+</sup> molecules (solid squares) and with MB<sup>+</sup>-GO complex (empty circles) at the delay time of 107 ps after the excitation. The blue solid lines represent GSB features of MB<sup>+</sup> in QD-MB<sup>+</sup> complex. The green dotted and solid lines represent bleaching features of CdSe QD and MB<sup>+</sup>-GO in QD-MB<sup>+</sup>-GO composite. The arrows represent the probe wavelengths for TA kinetic traces in QD-MB<sup>+</sup> and QD-MB<sup>+</sup>-GO composites. (b) TA kinetic traces in CdSe QDs with MB<sup>+</sup> molecules. The probe wavelength is 675 nm. (c) TA kinetic traces in CdSe QDs with MB<sup>+</sup>-GO complex. The probe wavelength is 610 nm. Left is linear scale and right is logarithmic scale in panels b and c.

The schematic illustration of photoinduced charge separation and recombination processes in composites of QD-MB<sup>+</sup> and QD-MB<sup>+</sup>-GO is shown in Figure 5. QD-MB<sup>+</sup> composite as a reference shows the typical charge separation and recombination processes, as seen in Figure 5a.<sup>17</sup> The electron transfer time from QD to MB<sup>+</sup> molecule was determined to be about 2 ps from the bleaching signal of CdSe 1S exciton state and GSB feature of MB<sup>+</sup>. The charge recombination lifetime was obtained to be about 600–700 ps by fitting the kinetic trace of GSB signal. In the hybrid system of CdSe QD-MB<sup>+</sup>-GO

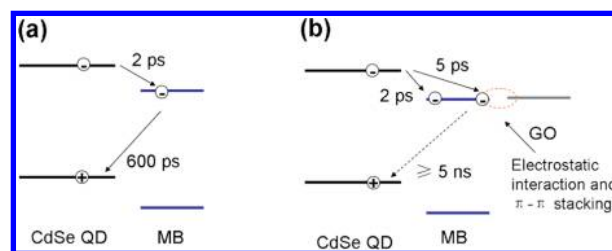


**Figure 5.** Schematic diagram of charge separation and recombination processes in CdSe QDs with MB<sup>+</sup> molecules (a) and MB<sup>+</sup>-GO complex (b). Red dotted circle represents electrostatic interaction and  $\pi$ - $\pi$  stacking between MB<sup>+</sup> and GO.

composite, the basic photophysical processes are unraveled through analysis of femtosecond TA spectra, as seen in Figure 5b. The electrostatic interaction and  $\pi$ - $\pi$  stacking induced absorption broadening and peak blue-shift are observed in steady-state and TA spectra. The electron transfer or energy transfer from MB<sup>+</sup> molecules to GO has been confirmed by PL quenching of MB<sup>+</sup>-GO complex. The charge separation lifetime of 1.8 ps from CdSe QDs to MB<sup>+</sup>-GO complex is similar to that in the QD-MB<sup>+</sup> composite. In the GO material functionalized by MB<sup>+</sup> molecule, the ability of GO to capture electrons is enhanced due to existence of MB<sup>+</sup> molecules as electron capture antenna. The rise time of 5.2 ps for the GSB signal in the MB<sup>+</sup>-GO complex is larger than the charge separation time (1.8 ps), which is attributed to the electron transfer from QD to GO via MB<sup>+</sup> as a bridge. On the other hand, the long charge recombination lifetime ( $\geq 5$  ns) is due to the weakened electronic coupling strength between radical and QD. However, the electrical conductivity of graphene oxide is very low ( $6 \times 10^{-5} \text{ S}\cdot\text{cm}^{-1}$ ) in contrast to RGO and graphene,<sup>41</sup> implying that the long-distance electron transport in GO is impossible. More recently, electron transfer from pyridine coated CdSe QDs to chemical vapor deposition (CVD)-fabricated single-sheet graphene was demonstrated.<sup>32</sup> We expect that the captured electron from QD can be transported fast along 2D network of graphene, due to its unique electrical properties, including excellent conductivity ( $10^6 \text{ S}\cdot\text{cm}^{-1}$ ) and high charge mobility ( $2 \times 10^5 \text{ cm}^2\cdot\text{V}^{-1}\cdot\text{s}^{-1}$ ).<sup>34</sup>

In conclusion, we have investigated photoinduced charge separation and recombination processes between CdSe QDs and MB<sup>+</sup> molecules-GO complex by femtosecond TA spectroscopy. The observed changes in steady-state and TA spectra of the QD-MB<sup>+</sup>-GO complex were attributed to MB<sup>+</sup> molecules anchored on the GO via electrostatic interaction and  $\pi$ - $\pi$  stacking interaction. Charge separation lifetime from CdSe QDs to MB<sup>+</sup>-GO complex was determined to be 1.8 ps. The rise time of the bleaching signal of MB<sup>+</sup>-GO complex was estimated to be 5.2 ps, which is longer than exciton dissociation time, because of electron transfer from QD to GO via MB<sup>+</sup> molecule as a bridge. Observation of very long charge recombination lifetime ( $\geq 5$  ns) in QD-MB<sup>+</sup>-GO composites indicates strong electronic coupling strength between MB<sup>+</sup>-GO radical and GO. The clear photophysical picture of charge separation and recombination at QD-MB<sup>+</sup>-GO interface obtained from this work may help for the future photovoltaic application of this sort of materials.

## ■ ASSOCIATED CONTENT

### ● Supporting Information

Experimental methods; photo images of MB<sup>+</sup> and MB<sup>+</sup>-GO before and after filtration in water; absorption, PL and FTIR spectra of MB<sup>+</sup> and MB<sup>+</sup>-GO; TEM images of CdSe QD with and without MB<sup>+</sup>, and CdSe QD-GO complex; TA spectrum of QD-MB<sup>+</sup>-GO; absorption, PL spectra, TA kinetic trace and PL decay of QD-GO; TA kinetic trace of QD-MB<sup>+</sup>-GO probed at 583 nm; simulated TA kinetic trace of QD-MB<sup>+</sup>-GO with fast rise time (1.8 ps). This material is available free of charge via the Internet <http://pubs.acs.org>.

## ■ AUTHOR INFORMATION

### Corresponding Author

\* (J.Z.) Phone: +86-431-86176313; e-mail: zhaojl@ciomp.ac.cn. (Y.M.) Phone: +81-298-534248; e-mail: masumoto@physics.px.tsukuba.ac.jp.

### Notes

The authors declare no competing financial interest.

## ■ ACKNOWLEDGMENTS

This work was supported by the National Natural Science Foundation of China (Nos. 11204298 and 11274304) and the Innovative Research Support Program (Pilot Model) of the University of Tsukuba, Japan.

## ■ REFERENCES

- (1) Greenham, N. C.; Peng, X.; Alivisatos, A. P. Charge Separation and Transport in Conjugated-Polymer-Semiconductor-Nanocrystal Composites Studied by Photoluminescence Quenching and Photoconductivity. *Phys. Rev. B* **1996**, *54*, 17628–17637.
- (2) Huynh, W. U.; Dittmer, J. J.; Alivisatos, A. P. Hybrid Nanorod–Polymer Solar Cells. *Science* **2002**, *295*, 2425–2427.
- (3) Sun, B. Q.; Marx, E.; Greenham, N. C. Photovoltaic Devices Using Blends of Branched CdSe Nanoparticles and Conjugated Polymers. *Nano Lett.* **2003**, *3*, 961–963.
- (4) Coe, S.; Woo, W. K.; Bawendi, M.; Bulović, V. Electroluminescence from Single Monolayers of Nanocrystals in Molecular Organic Devices. *Nature* **2002**, *420*, 800–803.
- (5) Zhao, J. L.; Bardecker, J. A.; Munro, A. M.; Liu, M. S.; Niu, Y. H.; Ding, I. K.; Luo, J. D.; Chen, B. Q.; Jen, A. K.-Y.; Ginger, D. S. Efficient CdSe–CdS Quantum Dot Light-Emitting Diodes Using a Thermally Polymerized Hole Transport Layer. *Nano Lett.* **2006**, *6*, 463–467.
- (6) Schaller, R. D.; Klimov, V. I. High Efficiency Carrier Multiplication in PbSe Nanocrystals: Implications for Solar Energy Conversion. *Phys. Rev. Lett.* **2004**, *92*, 186601(4).
- (7) Luther, J. M.; Beard, M. C.; Song, Q.; Law, M.; Ellingson, R. J.; Nozik, A. J. Multiple Exciton Generation in Films of Electronically Coupled PbSe Quantum Dots. *Nano Lett.* **2007**, *7*, 1779–1784.
- (8) Schaller, R. D.; Sykora, M.; Jeong, S.; Klimov, V. I. High-Efficiency Carrier Multiplication and Ultrafast Charge Separation in Semiconductor Nanocrystals Studied via Time-Resolved Photoluminescence. *J. Phys. Chem. B* **2006**, *110*, 25332–25338.
- (9) Beard, M. C.; Knutsen, K. P.; Yu, P.; Luther, J. M.; Song, Q.; Metzger, W. K.; Ellingson, R. J.; Nozik, A. J. Multiple Exciton Generation in Colloidal Silicon Nanocrystals. *Nano Lett.* **2007**, *7*, 2506–2512.
- (10) Midgett, A. G.; Luther, J. M.; Stewart, J. T.; Smith, D. K.; Padilha, L. A.; Klimov, V. I.; Nozik, A. J.; Beard, M. C. Size and Composition Dependent Multiple Exciton Generation Efficiency in PbS, PbSe, and PbS<sub>x</sub>Se<sub>1-x</sub> Alloyed Quantum Dots. *Nano Lett.* **2013**, *13*, 3078–3085.
- (11) Sambur, J. B.; Novet, T.; Parkinson, B. A. Multiple Exciton Collection in a Sensitized Photovoltaic System. *Science* **2010**, *330*, 63–66.
- (12) Semonin, O. E.; Luther, J. M.; Choi, S.; Chen, H. Y.; Gao, J. B.; Nozik, A. J.; Beard, M. C. Peak External Photocurrent Quantum Efficiency Exceeding 100% via MEG in a Quantum Dot Solar Cell. *Science* **2011**, *334*, 1530–1533.
- (13) Nair, G.; Bawendi, M. G. Carrier Multiplication Yields of CdSe and CdTe Nanocrystals by Transient Photoluminescence Spectroscopy. *Phys. Rev. B* **2007**, *76*, 081304(R).
- (14) Ben-Lulu, M.; Mocatta, D.; Bonn, M.; Banin, U.; Ruhman, S. On the Absence of Detectable Carrier Multiplication in a Transient Absorption Study of InAs/CdSe/ZnSe Core/Shell1/Shell2 Quantum Dots. *Nano Lett.* **2008**, *8*, 1207–1211.
- (15) Matylytsky, V. V.; Dworak, L.; Breus, V. V.; Basche, T.; Wachtveitl, J. Ultrafast Charge Separation in Multiexcited CdSe Quantum Dots Mediated by Adsorbed Electron Acceptors. *J. Am. Chem. Soc.* **2009**, *131*, 2424–2425.
- (16) Dworak, L.; Matylytsky, V. V.; Braun, M.; Basche, T.; Wachtveitl, J. Ultrafast Charge Separation at the CdSe–CdS Core-Shell Quantum Dot-Methylviologen Interface: Implications for Nanocrystal Solar Cells. *J. Phys. Chem. B* **2011**, *115*, 3949–3955.
- (17) Huang, J.; Huang, Z.; Yang, Y.; Zhu, H.; Lian, T. Multiple Exciton Dissociation in CdSe Quantum Dots by Ultrafast Electron Transfer to Adsorbed Methylene Blue. *J. Am. Chem. Soc.* **2010**, *132*, 4858–4864.
- (18) Zhu, H.; Lian, T. Enhanced Multiple Exciton Dissociation from CdSe Quantum Rods: The Effect of Nanocrystal Shape. *J. Am. Chem. Soc.* **2012**, *134*, 11289–11297.
- (19) Zhu, H.; Song, N.; Rodríguez-Córdoba, W.; Lian, T. Wave Function Engineering for Efficient Extraction of up to Nineteen Electrons from One CdSe–CdS Quasi-Type II Quantum Dot. *J. Am. Chem. Soc.* **2012**, *134*, 4250–4257.
- (20) Yang, Y.; Rodríguez-Córdoba, W.; Lian, T. Ultrafast Charge Separation and Recombination Dynamics in Lead Sulfide Quantum Dot–Methylene Blue Complexes Probed by Electron and Hole Intraband Transitions. *J. Am. Chem. Soc.* **2011**, *133*, 9246–9249.
- (21) Zhu, H.; Song, N.; Lian, T. Controlling Charge Separation and Recombination Rates in CdSe/ZnS Type I Core-Shell Quantum Dots by Shell Thicknesses. *J. Am. Chem. Soc.* **2010**, *132*, 15038–15045.
- (22) Židek, K.; Zheng, K.; Abdellah, M.; Lenngren, N.; Chábera, P.; Pullerits, P. Ultrafast Dynamics of Multiple Exciton Harvesting in the CdSe–ZnO System: Electron Injection versus Auger Recombination. *Nano Lett.* **2012**, *12*, 6393–6399.
- (23) Tagliazucchi, M.; Tice, D. B.; Sweeney, C. M.; Morris-Cohen, A. J.; Weiss, E. A. Ligand-Controlled Rates of Photoinduced Electron Transfer in Hybrid CdSe Nanocrystal–Poly(viologen) Films. *ACS Nano* **2011**, *5*, 9907–9917.
- (24) Adam, J.; Peterson, M. C.; M., D.; Frederick, M. T.; Kamm, J. M.; Weiss, E. A. Evidence for a Through-Space Pathway for Electron Transfer from Quantum Dots to Carboxylate-Functionalized Viologens. *J. Phys. Chem. Lett.* **2012**, *3*, 2840–2844.
- (25) Kamat, P. V. Graphene-Based Nanoassemblies for Energy Conversion. *J. Phys. Chem. Lett.* **2011**, *2*, 242–251.
- (26) Seger, B.; Kamat, P. V. Electrocatalytically Active Graphene-Platinum Composites. Role of 2-D Carbon Support in PEM Fuel Cells. *J. Phys. Chem. C* **2009**, *113*, 7990–7995.
- (27) Williams, G.; Seger, B.; Kamat, P. V. TiO<sub>2</sub>-Graphene Composites. UV-Assisted Photocatalytic Reduction of Graphene Oxide. *ACS Nano* **2008**, *2*, 1487–1491.
- (28) Kim, Y. T.; Shin, H. W.; Ko, Y. S.; Ahn, T. K.; Kwon, Y. U. Synthesis of a CdSe–Graphene Hybrid Composed of CdSe Quantum Dot Arrays Directly Grown on CVD–Graphene and Its Ultrafast Carrier Dynamics. *Nanoscale* **2013**, *5*, 1483–1488.
- (29) Lightcap, I. V.; Kamat, P. V. Fortification of CdSe Quantum Dots with Graphene Oxide. Excited State Interactions and Light Energy Conversion. *J. Am. Chem. Soc.* **2012**, *134*, 7109–7116.
- (30) Katsukis, G.; Malig, J.; Schulz-Drost, C.; Leubner, S.; Jux, N.; Guldi, D. M. Toward Combining Graphene and QDs: Assembling CdTe QDs to Exfoliated Graphite and Nanographene in Water. *ACS Nano* **2012**, *6*, 1915–1924.

- (31) Guo, C. X.; Yang, H. B.; Sheng, Z. M.; Lu, Z. S.; Song, Q. L.; Li, C. M. Layered Graphene–Quantum Dots for Photovoltaic Devices. *Angew. Chem., Int. Ed.* **2010**, *49*, 3014–3017.
- (32) Guo, S. R.; Bao, D. D.; Upadhyayula, S.; Wang, W.; Guvenc, A. B.; Kyle, J. R.; Hosseinibay, H.; Bozhilov, K. N.; Vullev, V. I.; Ozkan, C. S.; Ozkan, M. Photoinduced Electron Transfer Between Pyridine Coated Cadmium Selenide Quantum Dots and Single Sheet Graphene. *Adv. Funct. Mater.* **2013**, DOI: 10.1002-adfm.201203652.
- (33) Chen, D.; Feng, H. B.; Li, J. H. Graphene Oxide: Preparation, Functionalization, and Electrochemical Applications. *Chem. Rev.* **2012**, *112*, 6027–6053.
- (34) Dai, L. Functionalization of Graphene for Efficient Energy Conversion and Storage. *Acc. Chem. Res.* **2013**, *46*, 31–42.
- (35) Quintana, M.; Vazquez, E.; Prato, M. Organic Functionalization of Graphene in Dispersions. *Acc. Chem. Res.* **2013**, *46*, 138–148.
- (36) Bekyarova, E.; Sarkar, S.; Wang, F.; Itkis, M. E.; Kalinina, I.; Tian, X.; Haddon, R. C. Effect of Covalent Chemistry on the Electronic Structure and Properties of Carbon Nanotubes and Graphene. *Acc. Chem. Res.* **2013**, *46*, 65–76.
- (37) Wojcik, A.; Kamat, P. V. Reduced Graphene Oxide and Porphyrin. An Interactive Affair in 2-D. *ACS Nano* **2010**, *4*, 6697–6706.
- (38) Tachikawa, T.; Cui, S. C.; Fujitsuka, M.; Majima, T. Interfacial Electron Transfer Dynamics in Dye-Modified Graphene Oxide Nanosheets Studied by Single-Molecule Fluorescence Spectroscopy. *Phys. Chem. Chem. Phys.* **2012**, *14*, 4244–4249.
- (39) Liu, H.; Gao, J.; Xue, M.; Zhu, N.; Zhang, M.; Cao, T. Processing of Graphene for Electrochemical Application: Non-covalently Functionalize Graphene Sheets with Water-Soluble Electroactive Methylene Green. *Langmuir* **2009**, *25*, 12006–12010.
- (40) Treossi, E.; Melucci, M.; Liscio, A.; Gazzano, M.; Samori, P.; Palermo, V. High-Contrast Visualization of Graphene Oxide on Dye-Sensitized Glass, Quartz, and Silicon by Fluorescence Quenching. *J. Am. Chem. Soc.* **2009**, *131*, 15576–15577.
- (41) Xu, Y.; Bai, H.; Lu, G.; Li, C.; Shi, G. Flexible Graphene Films via the Filtration of Water-Soluble Noncovalent Functionalized Graphene Sheets. *J. Am. Chem. Soc.* **2008**, *130*, 5856–5857.
- (42) Swathi, R. S.; Sebastian, K. L. Resonance Energy Transfer from a Dye Molecule to Graphene. *J. Chem. Phys.* **2008**, *129*, 054703(9).
- (43) Klimov, V. I.; McBranch, D. W.; Leatherdale, C. A.; Bawendi, M. G. Electron and Hole Relaxation Pathways in Semiconductor Quantum Dots. *Phys. Rev. B* **1999**, *60*, 13740–13749.
- (44) Klimov, V. I.; Mikhailovsky, A. A.; McBranch, D. W.; Leatherdale, C. A.; Bawendi, M. G. Quantization of Multiparticle Auger Rates in Semiconductor Quantum Dots. *Science* **2000**, *287*, 1011–1013.
- (45) Karousis, N.; Sandanayaka, A. S. D.; Hasobe, T.; Economopoulos, S. P.; Sarantopoulou, E.; Tagmatarchis, N. Graphene Oxide with Covalently Linked Porphyrin Antennae: Synthesis, Characterization and Photophysical Properties. *J. Mater. Chem.* **2011**, *21*, 109–117.
- (46) Yan, Y. M.; Zhang, M. N.; Gong, K. P.; Su, L.; Guo, Z. X.; Mao, L. Q. Adsorption of Methylene Blue Dye onto Carbon Nanotubes: A Route to an Electrochemically Functional Nanostructure and Its Layer-by-Layer Assembled Nanocomposite. *Chem. Mater.* **2005**, *17*, 3457–3463.
- (47) Chagovets, V. V.; Kosevich, M. V.; Stepanian, S. G.; Boryak, O. A.; Shelkovsky, V. S.; Orlov, V. V.; Leontiev, V. S.; Pokrovskiy, V. A.; Adamowicz, L.; Karachevtsev, V. A. Noncovalent Interaction of Methylene Blue with Carbon Nanotubes: Theoretical and Mass Spectrometry Characterization. *J. Phys. Chem. C* **2012**, *116*, 20579–20590.
- (48) Ferrari, A. C.; Robertson, J. Interpretation of Raman Spectra of Disordered and Amorphous Carbon. *Phys. Rev. B* **2000**, *61*, 14095–14107.
- (49) Kudin, K. N.; Ozbas, B.; Schniepp, H. C.; Prud'homme, R. K.; Aksay, I. A.; Car, R. Raman Spectra of Graphite Oxide and Functionalized Graphene Sheets. *Nano Lett.* **2008**, *8*, 36–41.